# Total internal reflectance fluorescence reader for selective investigations of cell membranes

**Thomas Bruns**
Hochschule Aalen
Institut für Angewandte Forschung
Beethovenstrasse 1
73430 Aalen, Germany

**Wolfgang S. L. Strauss**
**Reinhard Sailer**
Universität Ulm
Institut für Lasertechnologien Medizin
und Messtechnik
Helmholtzstrasse 12
89081 Ulm, Germany

**Michael Wagner**
**Herbert Schneckenburger**
Hochschule Aalen
Institut für Angewandte Forschung
Beethovenstrasse 1
73430 Aalen, Germany
E-mail: herbert.schneckenburger@htw-aalen.de

**Abstract.** A novel setup for fluorescence measurements of surfaces of biological samples, in particular the plasma membrane of living cells, is described. The method is based on splitting of a laser beam and multiple total internal reflections (TIR) within the bottom of a microtiter plate (cell substrate), such that up to 96 individual samples are illuminated simultaneously by an evanescent electromagnetic field. Main prerequisites are an appropriate thickness and a high transmission of the glass bottom, which is attached to the 96-well cell culture plate by a noncytotoxic adhesive. Glass rods of rectangular cross sections are optically coupled to this bottom for TIR illumination. Fluorescence arising from the plasma membrane of living cells is detected simultaneously from all samples using an integrating charge-coupled device (CCD) camera. The TIR fluorescence reader is validated using cultivated cells incubated with different fluorescent markers, as well as stably transfected cells expressing a fluorescent membrane-associating protein. In addition, particularly with regard to potential pharmaceutical applications, the kinetics of the intracellular translocation of a fluorescent protein kinase c fusion protein upon stimulation of the cells is determined.  [DOI: 10.1117/1.2208617]

Keywords: fluorescence screening; total internal reflection illumination; plasma membrane; microtiter plate.

Paper 05366R received Dec. 6, 2005; revised manuscript received Feb. 7, 2006; accepted for publication Feb. 9, 2006; published online Jun. 7, 2006. This paper is a revision of a paper presented at the SPIE conference on Imaging, Manipulation, and Analysis of Biomolecules and Cells: Fundamentals and Applications, Jan. 2005, San Jose, California. The paper presented there appears (unrefereed) in SPIE Proc. Vol. 5699.

## 1 Introduction

For more than 20 years,[1] total internal reflection (TIR) of laser light has been used to study cell-substrate interfaces to receive more detailed information on cell membranes. When a light beam propagating through a medium of refractive index $n_1$ (e.g., glass) meets an interface with a second medium of refractive index $n_2 < n_1$ (e.g., cytoplasm), total internal reflection occurs at all angles of incidence $\Theta$, which are greater than a critical angle $\Theta_c = \arcsin(n_2/n_1)$. Despite being totally reflected, the incident beam establishes an evanescent electromagnetic field that penetrates into the second medium and decays exponentially with distance $z$ from the interface. According to the relation

$$d = (\lambda/4\pi)(n_1^2 \sin^2 \Theta - n_2^2)^{-1/2}, \quad (1)$$

penetration depths $d$ between about 60 nm and more than 300 nm are attained depending on the wavelength $\lambda$ and the angle of incidence $\Theta$. Therefore, fluorophores located within or close to the plasma membrane can be examined almost selectively in living cells. So far, total internal reflection fluorescence microscopy (TIRFM) has been applied for measuring the topography of cell-substrate contacts,[1–3] membrane,[4] or protein[5] dynamics, membrane-proximal ion fluxes,[6,7] endocytosis or exocytosis,[8–11] as well as membrane-associated photosensitizers.[12]

Meanwhile, TIRFM has been optimized for detection of very small sample volumes[13] and even single molecules.[14] However, only individual cases with multiple samples located on the surface of waveguides have been excited simultaneously by TIR.[15,16] High throughput or high content screening using fluorescence techniques would require simultaneous illumination of multiple samples, e.g., for drug discovery[17] or for examination of diseases accompanied by altered membrane properties, e.g., Morbus Alzheimer,[18] Morbus Crohn,[19] Niemann-Pick disease,[20] or Duchenne muscle dystrophy.[21]

For these purposes, we developed a microtiter plate reader system based on multiple TIR excitation and fluorescence detection. For basic validation of the system, cultivated U373-MG glioblastoma cells incubated with fluorescent membrane markers, as well as T47-D breast cancer cells stably transfected with a plasmid encoding for a plasma membrane-associating yellow fluorescent protein (EYFP-

Address all correspondence to Herbert Schneckenburger, Institut für Angewandte Forschung, Hochschule Aalen, Beethovenstrasse 1, Aalen, 73430 Germany; Tel: 49 7361 568 229; Fax: 49 7361 568 225; E-mail: herbert.schneckenburger@htw-aalen.de

1083-3668/2006/11(3)/034011/7/$22.00 © 2006 SPIE

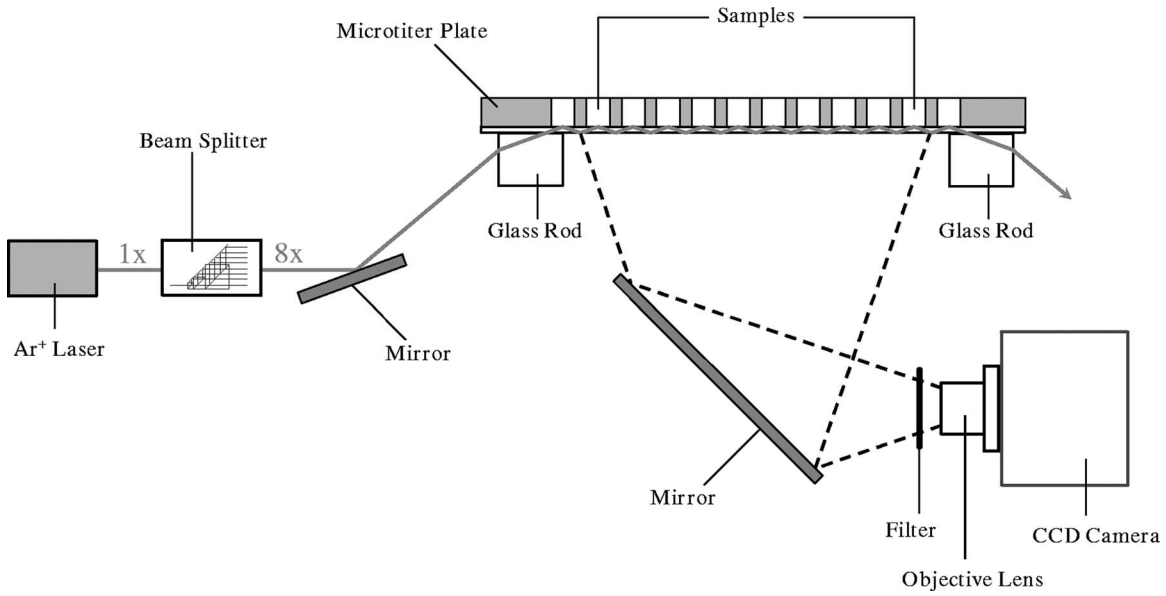


**Fig. 1** TIR fluorescence reader using 8× beamsplitting and 12-fold total internal reflection of each laser beam to illuminate 96 samples of a microtiter plate.

Mem), were used. In addition, as a biological model system for kinetic measurements, we used T47-D breast cancer cells stably transfected with a plasmid encoding for a fusion protein of protein kinase c and green fluorescent protein (PKC$\alpha$-EGFP), since activation of PKC by phorbol-12-myristate-13-acetate (PMA)[22] results in translocation of the protein toward the plasma membrane.

## 2 Materials and Methods

U373-MG human glioblastoma cells obtained from the European Collection of Cell Cultures (ECACC number 89081403) were routinely grown in RPMI 1640 culture medium supplemented with 10% fetal calf serum (FCS), glutamine, and gentamycin at 37 °C and 5% $CO_2$. After seeding of 500 cells/mm$^2$ within single cavities of a microtiter plate and a growth phase of 48 h, cells were incubated with RPMI medium (same as before) containing either the membrane marker 3,3'-dioctadecyloxacarbocyanine perchlorate (DiO) at a concentration of 8 $\mu$M (20 min) or the mitochondrial marker rhodamine 123 (R123) at variable concentrations between 5 and 15 $\mu$M (30 min). It has previously been shown that in this range of concentrations, R123 molecules are partly accumulated within the plasma membrane.[23] At the end of the incubation time, cells were washed and reincubated with phosphate buffered saline (PBS) prior to fluorometric measurements.

T47-D breast cancer cells, obtained from the American Type Culture Collection (ATTC, Rockville, Maryland) and stably transfected with the Living Colors™ subcellular localization vector pEYFP-Mem (Clontech, Palo Alto, California), were routinely cultivated in RPMI 1640 medium supplemented with 10% FCS and antibiotics at 37 °C and 5% $CO_2$. Cells were seeded at different densities in single cavities of a microtiter plate and grown for 48 h prior to fluorometric measurements. Furthermore, T47-D breast cancer cells were stably transfected with a plasmid encoding for a fluorescent PKC$\alpha$ fusion protein (pPKC$\alpha$-EGFP, Clontech, Palo Alto, California), which could be activated within the cell by phorbol-12-myristate-13-acetate (PMA). PMA was used at concentrations of 1, 10, or 100 nM in the culture medium (same as before) and incubated for up to 90 min. For T47-D as well as for U373-MG cells, subconfluent monolayers were obtained after a 48-h growth period.

As a light source, an air-cooled argon ion laser (model 5400B, Ion Lasers Technology, Salt Lake City, Utah) operated at $\lambda = 488$ nm and $P = 3$ mW was used together with a single mode fibre optic system, including collimating optics (kineFlex, Point Source, Southampton, United Kingdom) as well as a beamsplitter unit (consisting of a combination of three beam splitters and three mirrors), which divided the original laser beam into eight beams of almost identical intensity, 1 mm in diameter and a distance 9 mm between each other. As depicted in Fig. 1, each beam was incident on a rectangular glass rod that was optically coupled (by immersion oil) to the glass bottom of a microtiter plate. 96-well cell culture plates (without bottom and with a distance $s = 9$ mm between adjacent wells) were obtained from Greiner GmbH (Frickenhausen, Germany). Optiwhite glass bottoms of a thickness $d = 2$ mm and low absorbance (optical density $D = 0.045$ over a light path of 12 cm; Glaswerke Haller GmbH, Kirchlengern, Germany) were fixed on the plates using a noncytotoxic silicon adhesive (ALPA-SIL Extra, Alpina Technische Produkte GmbH, Germany). Cytotoxicity was assessed microscopically by comparison of cell growth when using either glass slides with various adhesives or control slides without adhesive. Adhesives were regarded to be noncytotoxic, if after a growth period of 48 h neither cell number nor cell morphology differed from that of control cells.

For multiple total internal reflections within the glass bottom, the angle of incidence $\Theta$ must be larger than the critical angle $\Theta_c$, which is about 64 deg, if refractive indices $n_1 = 1.525$ for the glass bottom and $n_2 = 1.37$ for the cells (cy-

toplasm) are assumed. To fulfil this requirement, the thickness $d=2$ mm of the plate was selected, such that $\Theta=\arctan(s/2d)=66$ deg was attained for the distance $s=9$ mm between the centers of two adjacent cavities of the plate. According to Eq. (1), a penetration depth of the evanescent field of about 150 nm into the culture medium of the cells was calculated. Since the Gaussian profile of the laser beam is preserved in the glass bottom, all samples of the microtiter plate exposed to the evanescent field are illuminated by an ellipse of 2.5 mm $\times$ 1 mm in diameter. The exciting laser light is coupled out of the glass bottom using a second glass rod of identical shape to avoid uncontrolled reflections. Fluorescence of the microtiter plate is detected simultaneously using an integrating digital charge-coupled device (CCD) camera (ProgRes C10, Jenoptik GmbH, Jena, Germany) together with a wide-angular objective lens (Cinegon 1.4/12–0.515, Schneider GmbH, Bad Kreuznach, Germany) and a long pass filter for $\lambda \geq 515$ nm, as depicted in Fig. 1. In some cases, an additional bandpass filter for $\lambda=529\pm25$ nm was used to reduce background luminescence of the glass plate. Exposure times varied between 2 and 60 s. Cavities without any cells or any dyes served as controls, and an average intensity obtained from those control wells was subtracted from the fluorescence values of all samples.

For analyzing fluorescence images of the microtiter plate (2080 $\times$ 1542 pixels), the whole images are split into matrices for individual samples of approximately 4000 elements each. Then, the intensity values of each matrix element are summed up such that the fluorescence of each sample is represented by a single value. Presently, eight samples on the left side and eight samples on the right side of the microtiter plate are excluded from evaluation, since these samples are partly covered by the glass rods. Fluorescence of the other 80 samples is analyzed, considering an adjustment of the slight differences in light intensity between the eight individual laser beams after splitting, as well as background subtraction (see earlier), but no further algorithms for data correction. This implies that currently no corrections are made concerning light absorption within the glass bottom or optical aberrations within the detection path.

In addition, for a microscopic assessment of the cell models, U373-MG cells, T47-D-EYFP-Mem cells, or T47-D-pPKC$\alpha$-EGFP cells were seeded on microscope slides (at a density of 150 cells/mm$^2$) and grown for 48 h under the same conditions as mentioned before. U373-MG cells were incubated with DiO or R123 as reported earlier. Fluorescence was collected using a 40 $\times$ 1.3 oil immersion objective lens and a long pass filter for $\lambda \geq 515$ nm. For illumination, again an argon ion laser operated at 488 nm was used in combination with single mode fiber optics as well as a custom-made dark field condenser permitting variable angles of illumination below or above the critical angle $\Theta_c$.[3] For detection of fluorescence images, an image intensifying camera system (Picostar HR12; LaVision, Göttingen, Germany)[4] operated in continuous wave mode was used.

## 3 Results

### 3.1 *Microscopic Assessment of the Cell Models*

For fluorescence microscopy, the angles of incidence of the illuminating laser beam were fixed at $\Theta=62$ deg for transillumination (whole cell measurements) and $\Theta=66$ deg for TIRFM (selective measurements of the plasma membrane and adjacent parts of the cytoplasm). Images of U373-MG cells incubated with DiO showed fluorescent intracellular filaments upon transillumination, and a fluorescent membrane area with some bright spots (supposed to be cell-substrate contacts) upon TIR illumination. Fluorescence images of U373-MG cells incubated with R123 showed a mitochondrial pattern at $\Theta=62$ deg and again some membrane-associated fluorescence at $\Theta=66$ deg (data not shown). Fluorescence images of T47-D-EYFP-Mem cells are depicted in Fig. 2 using again angles of incidence of 62 deg [Fig. 2(a)] and 66 deg [Fig. 2(b)] for illumination. In both cases, fluorescence mainly arises from the cell surface (plasma membrane), which appears as a sharp contour surrounding the cells at $\Theta=62$ deg and as a fluorescent area at $\Theta=66$ deg. Intracellular fluores-

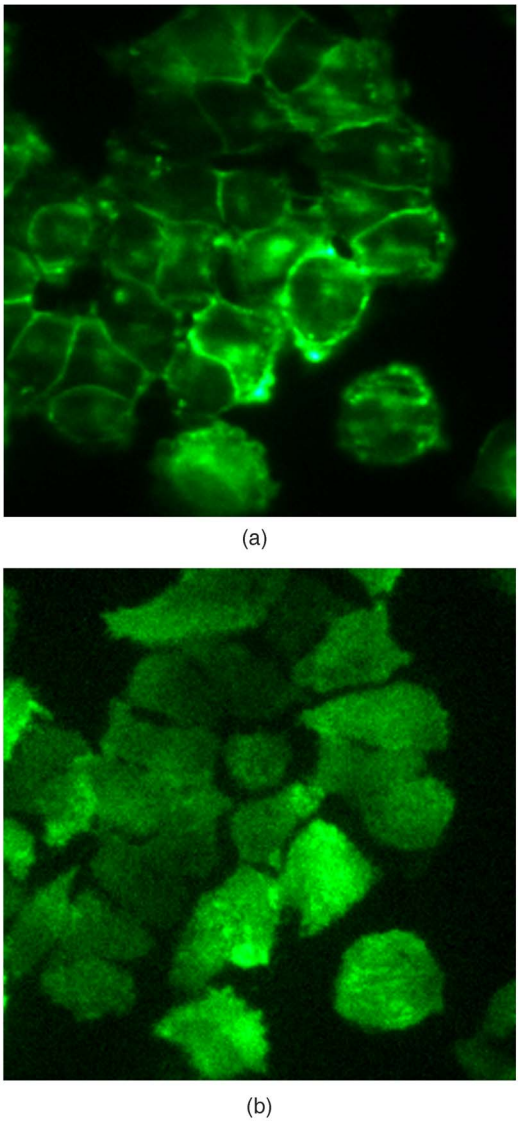

(a)

(b)

**Fig. 2** Fluorescence microscopy of T47-D-EYFP-Mem cells illuminated at $\Theta=62$ deg [(a) whole cell illumination] or at $\Theta=66$ deg [(b) TIR illumination] by an argon ion laser (488 nm). Fluorescence was measured at $\lambda \geq 515$ nm (image size 140 $\mu$m $\times$ 140 $\mu$m).

cence of untreated T47-D-PKC$\alpha$-EGFP cells (excited at $\Theta=62$ deg) was rather pronounced, whereas membrane-associated fluorescence (excited at $\Theta=66$ deg) appeared very weak and diffuse (data not shown). However, a considerable increase of membrane-associated fluorescence was observed upon application of PMA, resulting in brightly fluorescent cell surfaces at PMA concentrations of 100 nM and incubation times above 30 min. Therefore, TIR illumination appeared to be appropriate to examine the translocation of PKC$\alpha$-EGFP from the cytoplasm toward the plasma membrane upon PKC activation.

### 3.2 *Experiments for Validation of the Total Internal Reflectance Fluorescence Reader*

For validation of the TIR reader, the same cell models as reported before, i.e., incubated glioblastoma cells and stably transfected breast cancer cells, were used. Following incubation of U373-MG glioblastoma cells with the membrane marker DiO (8 $\mu$M) in 80 cavities of the microtiter plate, the fluorescence intensity was the same for all samples with a standard deviation of about ±10%. For U373-MG cells incubated with R123, the fluorescence signal increased linearly with R123 concentration within the measured range of 5 to 15 $\mu$M (correlation coefficient 0.9995). Again, standard deviations determined at 5, 10, and 15 $\mu$M (with 24 samples in each case) were around ±10% (data not shown).

Furthermore, T47-D-EYFP-Mem cells were seeded at different densities (125 or 250 or 500 cells/mm$^2$) into individual cavities of the microtiter plate. Cavities without any cells served as controls and were used for background correction, as mentioned earlier. As depicted in Fig. 3, the fluorescence intensity arising from the individual cavities reflects the number of seeded cells. This can be deduced from the fluorescence image of the microtiter plate [Fig. 3(a)] as well as from a quantitative evaluation of mean values and standard deviations of the samples of this plate [Fig. 3(b)] showing a virtually perfect linear relationship between the average fluorescence intensity and the number of cells (correlation coefficient 0.9994).

### 3.3 *Kinetic Measurements Using the Total Internal Reflectance Fluorescence Reader*

Similar to microscopic measurements, fluorescence of untreated T47-D-PKC$\alpha$-EGFP breast cancer cells appeared rather weak upon TIR illumination at $\Theta=66$ deg. Following PKC activation with PMA at a concentration of 10 or 100 nM, however, an increase of fluorescence intensity was observed due to translocation of the fluorescent fusion proteins from the cytosol toward the plasma membrane. In comparison with a PMA concentration of 10 nM, fluorescence increase was more pronounced at a concentration of 100 nM. Mean values and standard deviations obtained for the higher PMA concentration are depicted in Fig. 4 (resulting from eight wells of the microtiter plate and determined in intervals of 5 min up to 50 min, as well as in intervals of 10 min between 50 and 90 min after application of PMA). Fluorescence intensities were normalized for the values measured at 80 min, since at that time the absolute intensities were most similar and differed by less than 20% between each other. After some delay time, which is likely to reflect cellular uptake of the drug, TIR fluorescence shows a monotonous increase by about a factor of 8 during a time period of 10 to 60 min after PMA application, and an almost constant fluorescence signal thereafter. The time course of fluorescence intensity can fairly well be fitted by the function

$$I_F(t) = I_0 + (I_{max} - I_0) \times \{1 + \exp[-(t - t0)/\tau]\}^{-1}, \quad (2)$$

with the minimum intensity $I_0$, the maximum intensity $I_{max}$, the time constant $\tau$, as well the time $t_0$ at the point of inflexion when $I_F(t)$ is equal to $(I_0+I_{max})/2$. This fitting function is also depicted in Fig. 4. According to Eq. (2), $t_0=24.03$ min is calculated, and a fluorescence intensity corresponding to 90% of the maximum is attained at $t=53$ min after PMA application.

## 4 Discussion

Simultaneous excitation of surfaces of living cells by an evanescent electromagnetic field became possible by splitting a laser beam and by multiple total internal reflections (TIR) within a glass bottom of a microtiter plate. In each case, the angle of incidence $\Theta$ must be larger than the critical angle $\Theta_c$. This implies that at a given distance between individual samples, the glass bottom must have a defined thickness, e.g., 2 mm for a 96-well plate or 1 mm for a 384-well plate. In addition, light absorbance and scattering along the plate should be small, such that all samples are illuminated by similar intensities. In our case (using Optiwhite glass), an optical density of 0.045 was determined for a path length $l=12$ cm. Thus, laser intensity is reduced by about 10% when the beam is propagating along the whole plate and around 8% between the second and the 11th cavity of each row (as used in the present setup), respectively. Therefore, differences in laser irradiation up to ±4% presently contribute to the standard deviation of the measured values of about ±10%. However, in the future, differences of irradiation between individual samples could be eliminated by applying an appropriate correction algorithm.

In comparison with common window glass, where light intensity is reduced by about 45% over an optical path length of 12 cm (corresponding to an optical density of 0.26), light attenuation in Optiwhite glass is rather small and appears acceptable for the TIR reader. Special glass, quartz, or plastic materials of even lower attenuation are available, but seem to be either too expensive for routine applications or less favorable for TIR due to their comparably low refractive index. Attenuation of the propagating laser beam due to absorption of evanescent light by the samples is rather small. When assuming for each sample an absorber concentration of $c=10^4$ M, an extinction coefficient $\varepsilon=10^5$ L/(mol$\times$cm), and an absorbing layer that is thick compared with the penetration depth $d$ of the evanescent wave, the portion of absorbed light is $1.2\times10^{-3}$ per sample or 1.44% for 12 samples within one array. The influence of attenuation can be further reduced by reflection of laser light at the end of the glass plate, such that each sample is illuminated by two totally reflected laser beams with decreasing intensity from left to right for the incident beam, and from right to left for the reflected

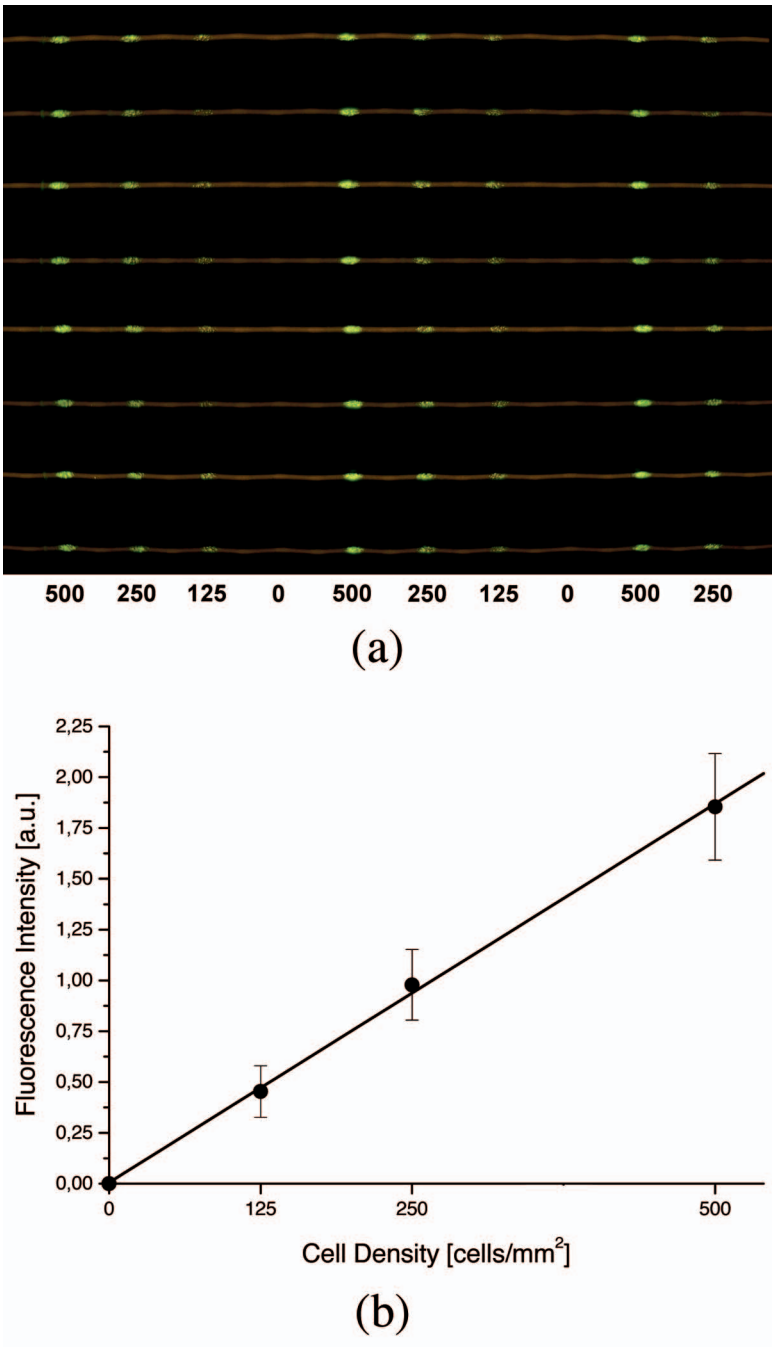


**Fig. 3** TIR fluorescence of T47-D-EYFP-Mem breast cancer cells seeded at different densities of 0, 125, 250, or 500 cells/mm$^2$ in a microtiter plate (excitation wavelength 488 nm; fluorescence detection 515 to 555 nm; recording time 60 s). (a) Image of the microtiter plate. (b) Quantitative evaluation: mean values ± standard deviations of 24 measurements (250 and 500 cells/mm$^2$) or 16 measurements (125 cells/mm$^2$).

beam. Beam reflection, however, needs very precise optical alignment, and multiple reflections may easily cause erroneous results.

As shown in the present work, TIR fluorescence was proportional to the concentration of fluorescent dyes used for incubation of the cells in the micromolar range as well as to the number of illuminated cells with membrane-associated fluorescent proteins. Assuming a doubling time of the T47D-EYFP-Mem cells of 24 h, about 1000, 2000, or 4000 cells were exposed to TIR illumination within each spot of the microtiter plate upon seeding of 125, 250, or 500 cells/mm$^2$, respectively, whereas about 17,500, 35,000, or 70,000 cells were contained within the whole cavities (6.5 mm in diameter). The fluorescence signal arising from about 1000 T47D-EYFP-Mem cells was by a factor of 4 larger than background luminescence, such that a minimum of a few 100 cells may be measured reliably. For quantification of the fluorescence signals, a rather homogenous distribution of cells in the cavities is necessary. Subconfluent cell layers may result in higher

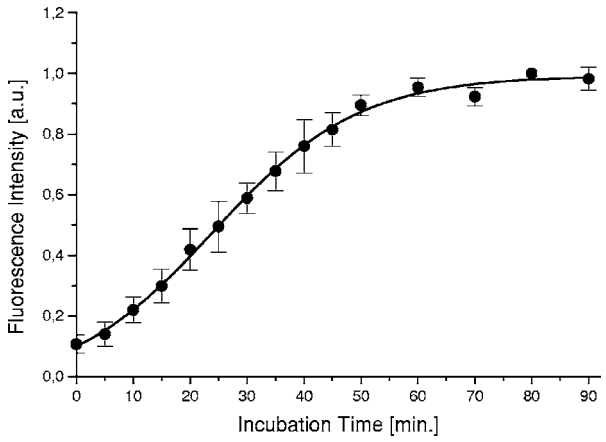


**Fig. 4** Time course of TIR fluorescence intensity of T47-D-PKC$\alpha$-EGFP breast cancer cells after incubation with 100-nM PMA in a microtiter plate (excitation wavelength 488 nm, fluorescence detection $\geq$515 nm; recording time 60 s; density of seeded cells 500 cells/mm$^2$). The mean values ± standard deviations of eight samples are shown as well as an approximation by the fitting function $I_F = I_0 + (I_{max} - I_0)\{1 + \exp[-(t - t0)/\tau]\}^{-1}$.

statistical spreading of the measured values than confluent cell layers, since the portion of illuminated cells within the wells may vary. Further problems arise if cells are growing as 3-D clusters or multilayers, which are not accessible to TIR illumination. The biological experiments reported before, however, indicate that those situations may be avoided if cell measurements are performed at standardized conditions, i.e., control of cell densities upon seeding and growth times between seeding and fluorescence measurements.

A further possibility to reduce statistical spreading in fluorescence measurements would be beam expansion, such that larger parts (up to about 50%) of the individual wells are illuminated. However, illumination by parallel light beams with a homogenous profile should be maintained, and light scattering at the edges of the wells has to be avoided in any case. This is achieved, e.g., by using lasers or laser diodes with single mode fibers and appropriate (possibly aspheric) telescope optics.

Detection devices should be sensitive enough for low photon fluxes. Assuming incident laser powers around 0.3 mW per well, about 0.3 $\mu$W are absorbed by each sample (corresponding to a flux of $7.5 \times 10^{11}$ photons per second). Assuming further a fluorescence quantum yield $\eta = 0.1$ and a solid angle of detection $\Omega = 0.1$ sr, the flux of fluorescence photons on the detector (arising from one well) is about $6 \times 10^8$ s$^{-1}$ (corresponding to a power of about 0.2 nW). Those low level signals can be detected when using charge-coupled device (CCD) cameras in an integrating mode with recording times of several seconds up to about one minute. It should be mentioned that fluorescence detection occurs preferentially on the bottom side of the multiwell plate, and that beam deflection (as depicted in Fig. 1) may be favorable to keep the instrument small. Image distortion by the wide-angular objective lens of the camera can be almost avoided, if the aperture of this lens (ratio of pupil diameter and focal length) is kept smaller than 0.5.

Determination of the kinetics of intracellular translocation of PKC$\alpha$ after stimulation with PMA proved that the TIR fluorescence reader can also be used for dynamic measurements, e.g., for assessment of cellular uptake of pharmaceutical agents, activation of signal transduction, or cytotoxic reactions. Signal acquisition and evaluation can be automated in these cases, such that the limiting factor will be the recording time for an individual image. When using an integrating CCD camera (as described before), a few seconds are needed for each image, such that the time resolution of kinetic measurements is presently limited to about 5 to 10 s. Further advances in camera technology may improve this time resolution in the near future.

In view of future applications of the TIR fluorescence reader for high throughput screening (HTS), it is essential to mention that microtiter plates can be easily exchanged without readjustment of the optical setup. In addition, due to the low penetration depth of the evanescent wave, only very small signals arising from cell culture media or supernatants are registered when using TIR illumination. Therefore, samples will become measurable in microtiter plates without any time-consuming washing procedures. More specific fluorescence parameters, i.e., spectra, lifetimes, or polarizations, can be obtained by replacing the CCD camera by appropriate detectors. Although this may require a scanning of the samples with a prolonged recording time, it results in a higher degree of information [high content screening (HCS)]. A combination of HTS and HCS appears valuable for the measurement of membrane dynamics based on spectral, polarization, or lifetime data, as already reported for fluorescence microscopy.[4]

## Acknowledgments

This project was supported by the Ministerium für Wissenschaft, Forschung und Kunst Baden-Württemberg. Technical assistance by Petra Kruse, Eva Winkler, and Claudia Hintze is gratefully acknowledged.

## References

1. D. Axelrod, "Cell-substrate contacts illuminated by total internal reflection fluorescence," *J. Cell Biol.* **89**, 141–145 (1981).
2. G. A. Truskey, J. S. Burmeister, E. Grapa, and W. M. Reichert, "Total internal reflection fluorescence microscopy (TIRFM) (2.) Topographical mapping of relative cell/substratum separation distances," *J. Cell. Sci.* **103**, 491–499 (1992).
3. K. Stock, R. Sailer, W. S. L. Strauss, M. Lyttek, R. Steiner, and H. Schneckenburger, "Variable-angle total internal reflection fluorescence microscopy (VA-TIRFM): realization and application of a compact illumination device," *J. Microsc.* **211**, 19–29 (2003).
4. H. Schneckenburger, M. Wagner, M. Kretzschmar, W. S. L. Strauss, and R. Sailer, "Laser-assisted fluorescence microscopy for measuring cell membrane dynamics," *Photochem. Photobiol. Sci.* **3**, 817–822 (2004).
5. S. E. Sund and D. Axelrod, "Actin dynamics at the living cell submembrane imaged by total internal fluorescence photobleaching," *Biophys. J.* **79**, 1655–1669 (2000).
6. G. M. Omann and D. Axelrod, "Membrane-proximal calcium transients in stimulated neutrophils detected by total internal reflection fluorescence," *Biophys. J.* **71**, 2885–2891 (1996).
7. A. Demuro and I. Parker, "Imaging the activity and localization of single voltage-gated $Ca^{2+}$ channels by total internal reflection fluorescence microscopy," *Biophys. J.* **86**, 3250–3259 (2004).
8. W. J. Betz, F. Mao, and C. B. Smith, "Imaging exocytosis and endocytosis," *Curr. Opin. Neurobiol.* **6**, 365–371 (1996).
9. M. Oheim, D. Loerke, D. W. Stuehmer, and R. H. Chow, "The last few milliseconds in the life of a secretory granule," *Eur. Biophys. J.* **27**, 83–98 (1998).

10. V. Beaumont, "Visualizing membrane trafficking using total internal reflection fluorescence microscopy," *Biochem. Soc. Trans.* **31**, 819–823 (2003).
11. M. W. Allersma, L. Wang, D. Axelrod, and R. W. Holz, "Visualization of regulated exocytosis with a granule-membrane probe using total internal reflection microscopy," *Mol. Biol. Cell* **15**, 4658–4668 (2005).
12. R. Sailer, W. S. L. Strauss, H. Emmert, K. Stock, R. Steiner, and H. Schneckenburger, "Plasma membrane associated location of sulfonated meso-tetraphenylporphyrins of different hydrophilicity probed by total internal reflection fluorescence spectroscopy," *Photochem. Photobiol.* **71**, 460–465 (2000).
13. T. Ruckstuhl and S. Seeger, "Attoliter detection volumes by confocal total-internal-reflection fluorescence microscopy," *Opt. Lett.* **29**, 569–571 (2004).
14. Y. Sako and T. Uyemura, "Total internal reflection fluorescence microscopy for single-molecule imaging in living cells," *Cell Struct. Funct* **27**, 357–356 (2002).
15. R. J. Obremski and J. W. Silzel, "System for simultaneously conducting multiple ligand binding assays," U.S. Patent No. 6,110,749 (2000).
16. A. Brandenburg, "Mikrooptische detektionssysteme für die bioanalytik," *Tech. Mess.* **68**, 513–518 (2001).
17. G. P. Sabbatini, W. A. Shirley, and D. L. Coffeen, "The integration of high throughput technologies for drug discovery," *J. Biomol. Screening* **6**, 213–218 (2001).
18. G. P. Eckert, N. J. Cairns, A. Maras, W. F. Gattaz, and W. E. Muller, "Cholesterol modulates the membrane-disordering effects of beta-amloyid peptides in the hippocampus: specific changes in Alzheimer's disease," *Dementia Geriatr. Cognit. Disord.* **11**, 181–186 (2000).
19. S. Aozaki, "Decreased membrane fluidity in erythrocytes from patients with Crohn's disease," *Gastroenterol. Jpn.* **24**, 246–254 (1989).
20. T. Koike, G. Ishida, M. Taniguchi, K. Higaki, Y. Ayaki, M. Saito, Y. Sakakihara, Y. Iwamori, and K. Onno, "Decreased membrane fluidity and unsaturated fatty acids in Niemann-Pick disease type C fibroblasts," *Biochim. Biophys. Acta* **1406**, 327–335 (1998).
21. C. Pasternak, S. Wong, and E. L. Elson, "Mechanical function of dystrophin in muscle cells," *J. Cell Biol.* **128**, 355–361 (1995).
22. S. Nakashima, "Protein kinase C alpha (PKC alpha): regulation and biological function," *J. Biochem. (Tokyo)* **132**, 669–675 (2002).
23. H. Schneckenburger, K. Stock, M. Lyttek, W. S. L. Strauss, and R. Sailer, "Fluorescence lifetime imaging (FLIM) of rhodamine 123 in living cells," *Photochem. Photobiol. Sci.* **3**, 127–131 (2004).